



A high-sensitive sensor and band-stop filter based on intersected double ring resonators in metal–insulator–metal structure

Abdesselam Hocini¹ · Hocine Ben salah^{1,2} · Djamel Khedrouche¹ ·
Noureddine Melouki¹

Received: 3 January 2020 / Accepted: 16 June 2020 / Published online: 28 June 2020
© Springer Science+Business Media, LLC, part of Springer Nature 2020

Abstract

In this paper, a waveguide coupled with two intersected cavity ring resonators, based plasmonic sensor has been proposed, which is compact in design with higher sensitivity. The structural parameters of the sensor has a key role in its sensitivity and transmission spectrum, and are analyzed using the finite-difference time-domain method embedded in the commercial simulator Rsoft. The results yield a linearity between the refractive index of the material under testing and its resonance wavelengths. The maximum achieved linear sensitivity was $S = 2448 \text{ nm/RIU}$ for the second mode and $S = 1120 \text{ nm/RIU}$ for the first mode, its corresponding sensing resolution is $4.08 \times 10^{-6} \text{ RIU}$ for mode 2 and $8.98 \times 10^{-6} \text{ RIU}$ for mode 1, which makes our design a promising candidate for high performance nano-sensors and bio-sensing devices. It's also applicable as a band-stop filter, due to the fact that the positions of transmission peaks and bandwidth can be easily manipulated, by adjusting both the inner radius and the distance between the centers of the two ring resonators.

Keywords Surface plasmon polaritons (SPP) · Metal insulator–metal (MIM) waveguide · Refractive index sensor · Band-stop filter · Intersected double ring resonators

✉ Abdesselam Hocini
abdesselam.hocini@univ-msila.dz

Hocine Ben salah
hocine.bensalah@univ-msila.dz

Djamel Khedrouche
djamel.khedrouche@univ-msila.dz

Noureddine Melouki
noureddine.melouki@univ-msila.dz

¹ Laboratoire d'Analyse des Signaux et Systèmes, Department of Electronics, University of M'Sila, BP. 166 Route Ichebilia, 28000 M'sila, Algeria

² Université Yahia fares Médéa, Médéa, Algeria

1 Introduction

Optical signal processing circuits suffer from the diffraction limit of the light, in the classical photonics, it keeps the size of light processing components at least an order of magnitude larger than the size of the electrical counterpart. In classical photonics, the changes in the optical parameters of the materials under testing, enables a modulation in a form of an electro–optical effect, which is not as strong to be used on a chip. This inconvenience motivates a search for novel materials and structures to overcome it (Stockman 2018).

Plasmonic structures with their unique capabilities to guide and manage light at below diffraction limit by using surface plasmon polaritons (SPP), have been widely used, due to the effect of the incident electromagnetic field in the continuous dielectric and free electrons in metal, where the SPP are the excited waves on the metal surface; they concentrate their energies in nanometer scale, which led to overcoming the classical optical diffraction limit (Ben salah et al. 2019).

Many devices based on SPP phenomena were designed and proposed such as the sensor in Binfeng (2014), where the authors proposed a metal–insulator–metal plasmonic Bragg grating based sensor, and as for the authors of Lu (2012), the nano-sensor was based on fano resonance in waveguide-coupled resonators. Wang et al. (2017) shows that diffraction limit can be overcome in nano-lasers by exploiting this phenomena. In Huang (2014) aside from using such structures as nano-sensors, the authors used it also as a fast-tunable filter based on guided-plasmonic wave resonance on a curved graphene surface. Many other devices were also proposed and designed on the SPP phenomena such as the couplers in Han et al. (2006), and the photo detector and the optical switches in Fang (2013); Gómez-Díaz and Perruisseau-Carrier (2013).

One of the most basic plasmonic waveguide structures, where light can be confined in a considerable propagating length is the metal–insulator–metal (MIM) based waveguide structure. In addition to that, many applications were based on a sub wavelength MIM waveguides coupled to one or more cavities (Paul and Ray 2016), with different types of the plasmonic sensors and filters such as the nanodisk resonators proposed by the authors of Guoxi (2011), and the tooth shaped waveguide (Zheng 2013).

Plasmonic ring resonators attracted the attention in recent years, as vital components in the integrated circuits, due to their compactness, high-quality factor, and ease of fabrication (Nezhad et al. 2013; Zhang 2018; Rakhshani and Mansouri-Birjandi 2016; Xiang and Li 2014; Yin et al. 2018; Rafiee et al. 2014). Adjusting the geometric parameters of the ring resonator tunes the resonance frequencies accordingly (Chen 2014; Janipour 2013).

To better understand and analyze a sensor's performance, the sensitivity is one of the most important properties to do so, by studying the effects of changing the refraction index in different materials under testing. Therefore, the objective is to improve the sensitivity by applying different design topologies in a small area, and exploiting the advantage of tuning the resonance frequencies by geometrical changes in ring resonator based structures such as the one presented in this work.

In this study, an MIM based waveguide coupled with the stub and double intersected ring resonators structure, is proposed as a plasmonic refractive index nano-sensor and a band-stop filter. The perfectly matched layer absorbing boundary condition is applied and the calculations were carried out using the finite-difference time-domain (FDTD) method implemented in the commercial simulator Rsoft, we varied the distance between the center of the two ring resonators, and their inner radius, to study the effect of the parameters changes on its sensing characteristics and refractive index sensitivity. From the results we

found, our proposed design is a promising candidate for both a high sensitivity sensor and a band-stop filter.

2 Design and analysis method

The schematic of the MIM plasmonic structure is shown in Fig. 1. It is composed of a slit and two identical intersected rings. The width of the waveguide, the distance between the ring resonator and the waveguide, the distance between the centers of the two ring resonators, are denoted as w , g and d , respectively. The inner and outer radiuses of the ring are defined as r and R , respectively. The width of the waveguide w is 50 nm, so the only excited mode is (TM_0) in the MIM waveguides (Gai et al. 2007). The gray and white areas represent the silver layer and the dielectric material, respectively.

The frequency dependent dielectric constant of silver is expressed by Lorentz–Drude model (Taflove and Hagness 2005):

$$\epsilon_m(\omega) = \epsilon_\infty - \frac{\omega_p^2}{\omega(\omega + i\gamma)} \tag{1}$$

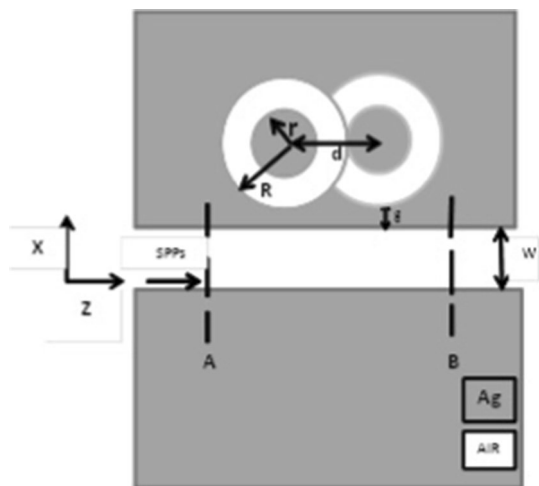
where ϵ_∞ is the dielectric constant at the infinite angular frequency with a value of 3.7, ω_p is the bulk plasma frequency ($\omega_p = 1.38 \times 10^{16} Hz$), and γ is the electron collision frequency ($\gamma = 2.73 \times 10^{13} Hz$) and ω is the angular frequency of the incident wave in vacuum (Zafar and Salim 2015).

In our simulation scenario, the magnetic field is parallel to y axis since the incident light for excitation of the SPP mode is TM-polarized (Wei 2005). The resonance wavelength of the ring resonator can be approximately given by the following (Guo 2018):

$$\lambda_m = \frac{2Re(\eta_{eff})L_{eff}}{m}, \quad m = 1, 2, 3, \dots \tag{2}$$

where $L_{eff} = \pi(r + R)$ is the effective resonance length, $Re(\eta_{eff})$ is the real part of the effective refractive index of the SPP.

Fig. 1 Schematic diagram of the MIM plasmonic structure



The implemented FDTD method using Rsoft commercial software (Zhang 2009), with the imposed condition of Perfectly Matched Layers (PML) as the absorbing boundary condition for all sides of the computational window to absorb outgoing waves, is applied on the structure to simulate its transmission characteristics. The grid size in both the x and z directions are chosen as $\Delta_x = \Delta_z = 5 \text{ nm}$ (Ben salah et al. 2019). The input type is a continuous Gaussian modulated wave of TM polarization field. The transmitted light was collected from the right side of the waveguide which is defined as $T = P_{out}/P_{in}$. Both the incident power P_{in} and the transmitted power P_{out} are observed at positions A and B.

When designing a surface plasmon resonance (SPR) based sensor, the sensitivity (S), is an important parameter and aspect, and it can be calculated as $S = \Delta_\lambda/\Delta_n$ (nanometer per refractive index (nm/RIU)) (Wu 2014), where Δ_λ denotes the shifting rate of resonant peak wavelength of transmittance, and Δ_n represents the changing rate in the refraction index in the plasmonic sensor structure.

The structural parameters are set to be $R = 450 \text{ nm}$, $r = 120 \text{ nm}$, $g = 10 \text{ nm}$ and $d = 100 \text{ nm}$, respectively.

3 Numerical results and discussion

First, the refractive index n of the insulator in the dielectric core and cavities is assumed to be 1. As we can see in Fig. 2a, the two transmission peaks are observed at the resonance wavelengths of $0.7054 \mu\text{m}$ for mode 1 and $1.3816 \mu\text{m}$ for mode 2, concerning single ring resonator, and $0.8238 \mu\text{m}$ for mode 1 and $1.6696 \mu\text{m}$ for mode 2, concerning the double intersected ring resonators, it is clearly seen that the existence of intersected double ring, results in red shift of resonance wavelengths and an increase in the devices's transmission by 32 % for mode 2, and 12.5 % for mode 1.

In Fig. 2b, the resonance wavelength is $1.3816 \mu\text{m}$ for the MIM plasmonic structure coupled with a single ring resonator (left). However, when the MIM based sensor is coupled with a double ring resonators, there is no resonance at $1.3816 \mu\text{m}$ wavelength(center), but the structure is resonating at $1.6696 \mu\text{m}$ (right). So a noticeable increase in the resonance wavelength, when the MIM plasmonic sensor is coupled with double ring resonators.

Figure 3 depicts the field distributions of $|H_y|$ for the on and off resonance wavelengths of the proposed structure. It's clear that the incident light with the wavelength of $0.8238 \mu\text{m}$ and $1.6696 \mu\text{m}$, couples to the double ring resonator and it's prohibited to pass through the waveguide, while the rest of the wavelengths are transmitted to the output.

Figure 4 illustrates the effect of the coupling distance g , so when an increase in this latter's value, a transmission level with no shift of resonances wavelengths is achieved. In addition, the maximum transmittances are reduced accordingly, due to the fact that the MIM coupler losses are increased also with increasing of the distance g (Zhao et al. 2008).

In Fig. 5a the transmission spectra of the proposed design for different refractive indices varying from 1 to 1.2 in steps of 0.05 is depicted, where it's noted that when an increasing in the refractive index n is occurred, results in a red-shift of resonance wavelengths of the transmitted spectra, with a larger shift in mode 2 in comparison to mode 1.

Figure 5b represents the maintained linearity between the resonance wavelengths and the refractive indices for both the first and the second modes, with the single ring and the intersected double ring resonators. Also, the achieved resonance wavelengths of the MIM based plasmonic sensor structure with the intersected double ring resonators, are greater than of those with the single ring resonator MIM based plasmonic sensor.

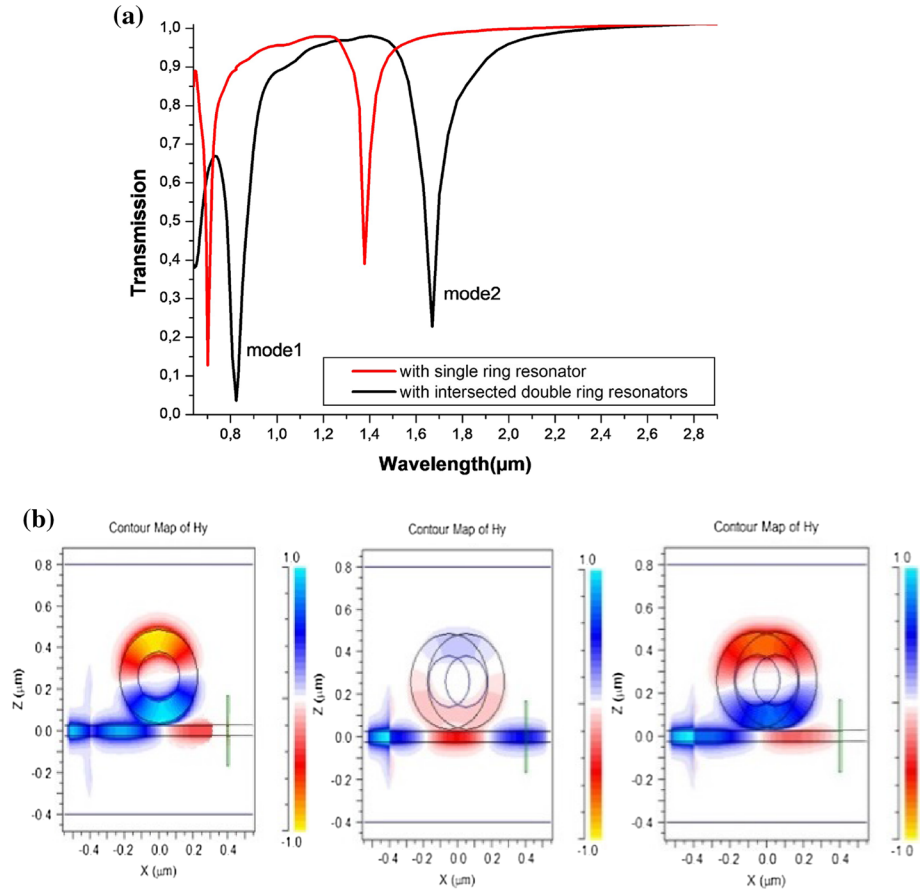


Fig. 2 **a** The transmission spectra of MIM plasmonic waveguides coupled with single ring and intersected double ring resonators with $n = 1$, $R = 450$ nm, $r = 120$ nm, $g = 10$ nm and $d = 100$ nm. **b** Magnetic-field patterns of the MIM plasmonic structure (left) with single ring at resonance wavelength $1.3816 \mu\text{m}$. (center) with intersected double ring at wavelength $1.3816 \mu\text{m}$. (right) with intersected double ring at resonance wavelength $1.6696 \mu\text{m}$

While keeping the other existing parameters fixed, and increasing the refraction index from $n = 1$ to 1.2, the sensitivity for the first mode is around 806 nm/RIU and for the second mode is around 1606 nm/RIU for MIM based plasmonic sensor with intersected double ring resonators, and 665 nm/RIU for mode 1 and 1440 nm/RIU for mode 2 in the case of a single ring resonator MIM plasmonic structure. It is clearly seen that, the existence of the intersected double ring structure, results in an increase in the device's sensitivity by 11.5 % for mode 2 and 21.2 % for mode 1.

Figure 6, illustrates the effect of the distance between the centers of the two ring resonators, where an increase in the value of d from 50 to 200 nm with a step of 50 nm is associated with an increase in resonance wavelength. Meaning, the value of d causes a shift in resonance wavelength, and the shift for mode 2 is larger than that for mode 1 as shown in Fig. 6a. There is a linear relation to be noted, between the wavelength resonances and the refractive indices as illustrated in Fig. 6b, despite the increase in the value of the distance

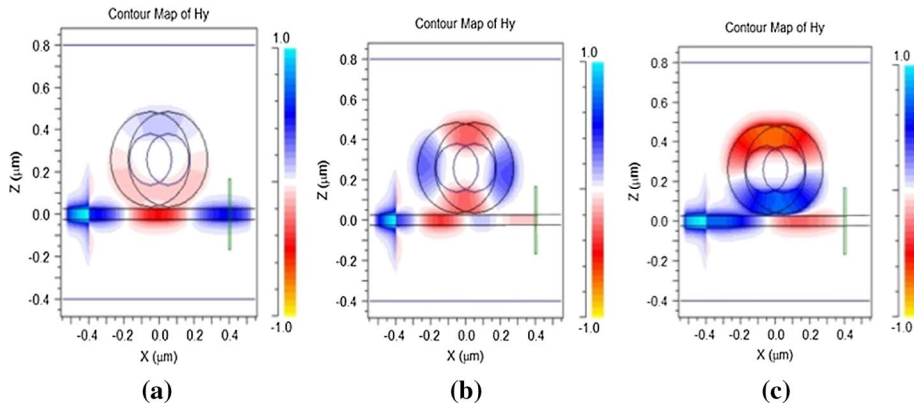


Fig. 3 Magnetic-field patterns of the MIM plasmonic waveguides coupled with intersected double ring at wavelength of **a** $1.2 \mu\text{m}$, and resonance wavelengths of **b** $0.8238 \mu\text{m}$, **c** $1.6696 \mu\text{m}$

Fig. 4 The transmission spectrum of the structure versus wavelength with different coupling distance g at $n = 1$, $R = 450 \text{ nm}$, $r = 120 \text{ nm}$ and $d = 100 \text{ nm}$

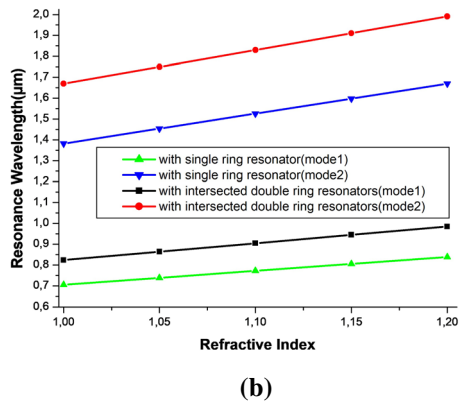
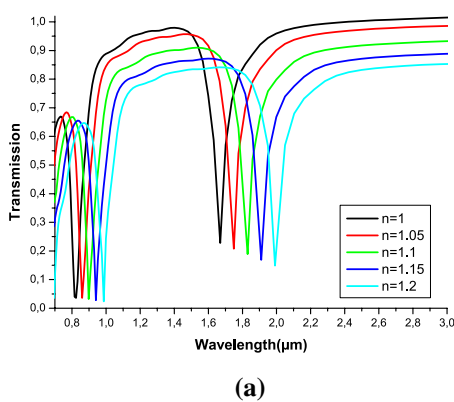
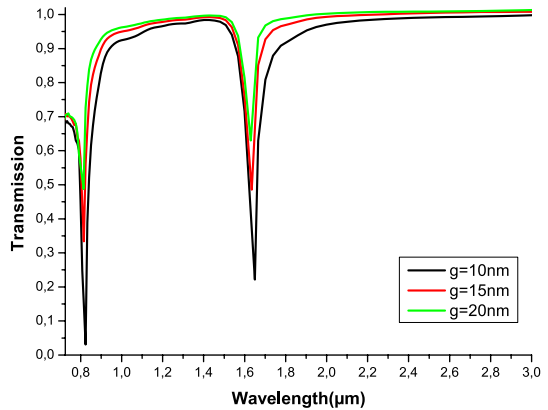


Fig. 5 a The transmission spectrum of the structure for different refractive index n at $R = 450 \text{ nm}$, $r = 120 \text{ nm}$, $g = 10 \text{ nm}$ and $d = 100 \text{ nm}$. **b** the resonance wavelength versus the refractive index n of the material under sensing

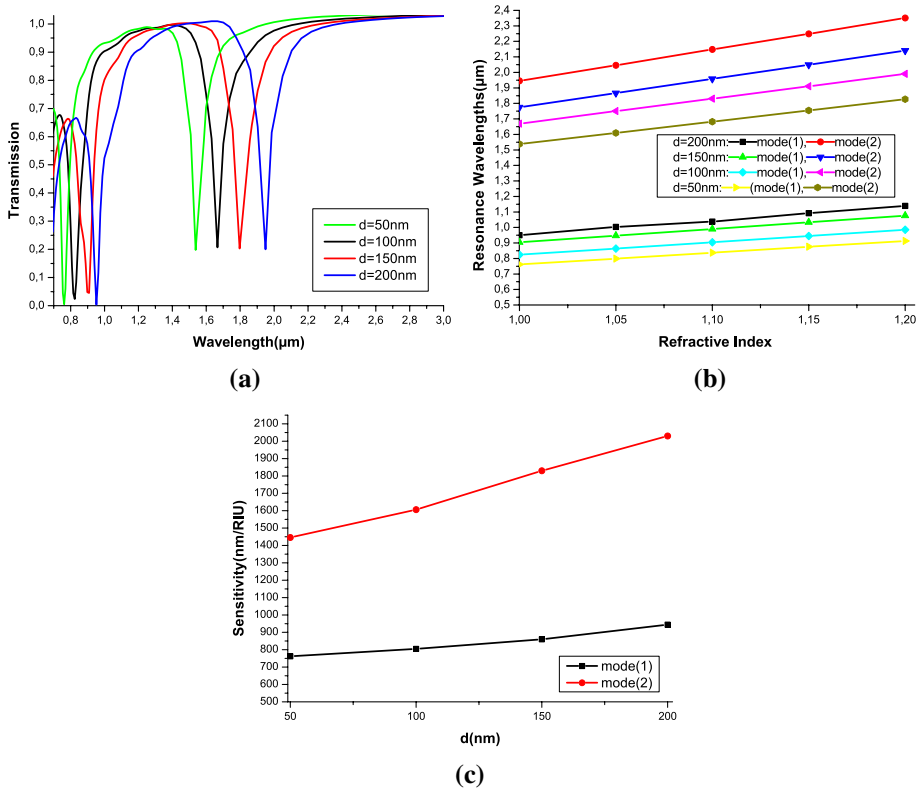


Fig. 6 Sensing properties as functions of *d*. **a** Transmission spectra of index 1 for *d* varying from 50 to 200 nm. **b** The resonance wavelengths versus the refractive index for different *d*. **c** Sensitivities of the plasmonic sensors for *d* varying from 50 to 200 nm

d. In addition to the fact that, the greater the value of *d* (50 nm to 200 nm) is, the higher the sensitivity of the sensor. The best achieved sensitivities are 944 nm/RIU and 2030 nm/RIU, So an improvement of 182 nm/RIU and 584 nm/RIU for both mode 1 and mode 2 respectively, i.e. sensing resolution of 1.06×10^{-5} RIU for mode1 and 4.92×10^{-6} RIU for mode2, can be achieved when the value *d* = 200 nm. From Fig. 6c it is noted that the relation between the sensitivity and the value *d* is almost linear, and the best achieved sensitivity is when *d* = 200 nm.

Next, we analyzed the impact of different values of *r* on the plasmonic refractive index sensor's properties, *d* is fixed with the best previously found value of 200 nm for next analysis. Transmission spectra of index 1 for values of *r* varying from 100 to 160 nm in steps of 20 nm are demonstrated in Fig. 7a, the increase in value *r* is associated with an increase in resonance wavelength. Meaning, the value of *r* causes a shift in resonance wavelength, and the shift for mode 2 is larger than that for mode 1 due to larger losses. From Fig. 7b it's clearly noted that the linearity is maintained in spite of the increase in the value of *r*. In addition to that, an enhancement of the sensor's sensitivity is achieved by increasing the value of *r*, for mode 1 the sensitivity is 1120 nm/RIU whereas in the case of mode 2, the sensitivity was 2448 nm/RIU, i.e. sensing resolution of 8.98×10^{-6} RIU for mode1 and 4.08×10^{-6} RIU for mode2, is achieved

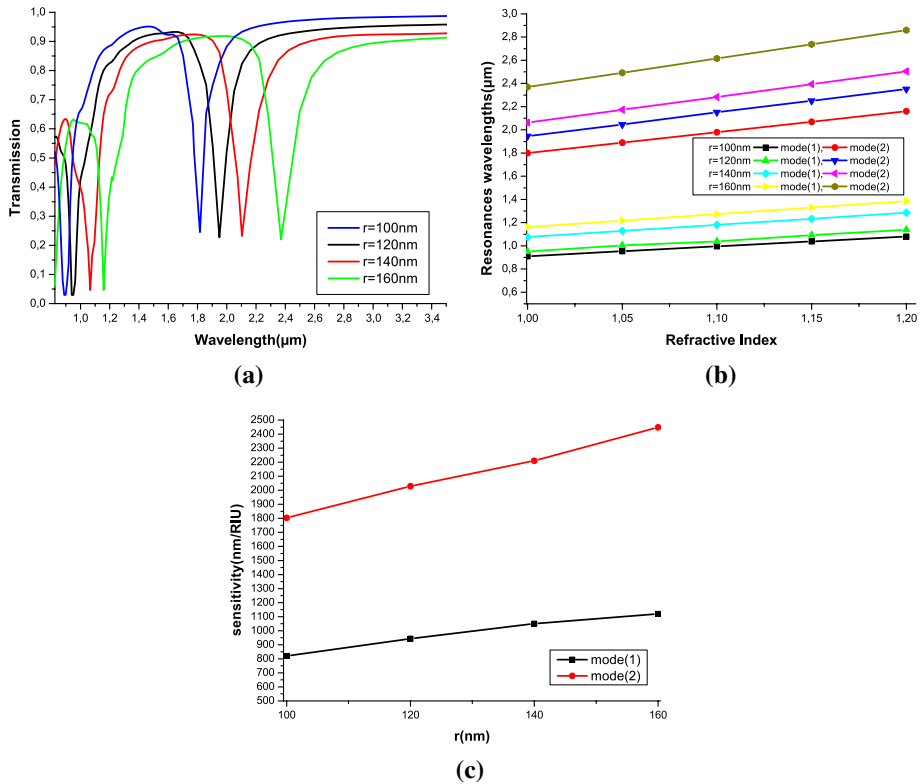


Fig. 7 Sensing properties as functions of r . **a** Transmission spectra of index 1 for r varying from 100 to 160 nm. **b** The resonance wavelengths versus the refractive index for different r . **c** Sensitivities of the plasmonic sensors for r varying from 100 to 160 nm

corresponding to value of $r = 160$ nm, in comparison to sensitivity of 820 nm/RIU for mode1 and 1804 nm/RIU for mode2 where the value of r was 100 nm. In Fig. 7c it is clearly shown that the greater the value of r is, the better the sensor’s performance.

Table 1 compares the sensitivity (S) of our proposed structure in comparison to other MIM plasmonic sensors in the literatures.

Table 1 Sensitivity comparison of different sensor structures

References	Sensitivity (nm/RIU)	Year
Yan et al. (2017)	1071.4	2017
Zhang (2018)	1060	2018
Ghorbani et al. (2018)	1540 for mode 2 and 1010 for mode 1	2018
Chou Chau (2019)	8280	2019
Ben salah et al. (2019)	2602.5	2019
In this work	2448 for mode 2 and 1120 for mode 1	2019

4 Conclusion

An MIM waveguide coupled with double intersected cavity ring resonators, is analyzed using the finite-difference time-domain (FDTD) method based analysis environment for a refractive index sensor. The transmission dips positions have linear relations in respect to the refractive index. In addition, in this proposed structure, and after optimizing its structural parameters, the maximum achieved linear sensitivity is $S = 2448 \text{ nm/RIU}$ and $S = 1120 \text{ nm/RIU}$ for both mode 2 and mode 1 respectively, this structure can also be used as band-stop filter, since the positions of transmission peaks and bandwidth can be easily manipulated by adjusting the inner radius of the ring resonators and the distance between the centers of these later. And this makes our proposed design an attractive candidate for both a nano-sensor and a stop-band filter.

Acknowledgements This work was supported by the Algerian Ministry of Higher Education and Scientific Research and La Direction Générale de la Recherche Scientifique et du Développement Technologique (DGRSDT) via funding through the PRFU Project No. A25N01UN28012 0180001.

References

- Ben salah, H., Hocini, A., Temmar, M.N., Khedrouche, D.: Design of mid infrared high sensitive metal-insulator-metal plasmonic sensor. *Chin. J. Phys.* **61**, 86–97 (2019)
- Binfeng, Y., et al.: Design of a compact and high sensitive refractive index sensor base on metal-insulator-metal plasmonic Bragg grating. *Opt. Express* **22**(23), 28662–28670 (2014)
- Chen, J., et al.: Tunable resonances in the plasmonic split-ring resonator. *IEEE Photonics J.* **6**(3), 1–6 (2014)
- Chou Chau, Y.-F., et al.: Ultra-high refractive index sensing structure based on a metal-insulator-metal waveguide-coupled T-shape cavity with metal nanorod defects. *Nanomaterials* **9**(10), 1433 (2019)
- Fang, Z., et al.: Active tunable absorption enhancement with graphene nanodisk arrays. *Nano Lett.* **14**(1), 299–304 (2013)
- Gai, H., Wang, J., Tian, Q.: Modified Debye model parameters of metals applicable for broadband calculations. *Appl. Opt.* **46**(12), 2229–2233 (2007)
- Ghorbani, S., Dashti, M.A., Jabbari, M.: Plasmonic nano-sensor based on metal-dielectric-metal waveguide with the octagonal cavity ring. *Laser Phys.* **28**(6), 066208 (2018)
- Gómez-Díaz, J.-S., Perruisseau-Carrier, J.: Graphene-based plasmonic switches at near infrared frequencies. *Opt. Express* **21**(13), 15490–15504 (2013)
- Guo, Z., et al.: Plasmonic multichannel refractive index sensor based on subwavelength tangent-ring metal-insulator-metal waveguide. *Sensors* **18**(5), 1348 (2018)
- Guoxi, W., et al.: Optical bistability in metal-insulator-metal plasmonic waveguide with nanodisk resonator containing Kerr nonlinear medium. *Appl. Opt.* **50**(27), 5287–5290 (2011)
- Han, Z., Liu, L., Forsberg, E.: Ultra-compact directional couplers and Mach-Zehnder interferometers employing surface plasmon polaritons. *Opt. Commun.* **259**(2), 690–695 (2006)
- Huang, Z.-R., et al.: A mid-infrared fast-tunable graphene ring resonator based on guided-plasmonic wave resonance on a curved graphene surface. *J. Opt.* **16**(10), 105004 (2014)
- Janipour, M., et al.: A novel adjustable plasmonic filter realization by split mode ring resonators. *J. Electromagn. Anal. Appl.* **5**(12), 40602 (2013)
- Lu, H., et al.: Plasmonic nanosensor based on Fano resonance in waveguide-coupled resonators. *Opt. Lett.* **37**(18), 3780–3782 (2012)
- Nezhad, V.F., Abaslou, S., Abrishamian, M.S.: Plasmonic band-stop filter with asymmetric rectangular ring for WDM networks. *J. Opt.* **15**(5), 055007 (2013)
- Paul, S., Ray, M.: Analysis of plasmonic subwavelength waveguide-coupled nanostub and its application in optical switching. *Appl. Phys. A* **122**(1), 21 (2016)
- Rafiee, E., Emami, F., Nozhat, N.: Coupling coefficient increment and free spectral range decrement by proper design of microring resonator parameters. *Opt. Eng.* **53**(12), 123108 (2014)

- Rakhshani, M.R., Mansouri-Birjandi, M.A.: High-sensitivity plasmonic sensor based on metal–insulator–metal waveguide and hexagonal-ring cavity. *IEEE Sens. J.* **16**(9), 3041–3046 (2016)
- Stockman, M.I., et al.: Roadmap on plasmonics. *J. Opt.* **20**(4), 043001 (2018)
- Taflove, A., Hagness, S.C.: *Computational Electrodynamics: The FiniteDifference Time-Domain Method*, 3rd edn. Artech House, Boston (2005)
- Wang, S., et al.: Unusual scaling laws for plasmonic nanolasers beyond the diffraction limit. *Nat. Commun.* **8**, 1889 (2017)
- Wei, P.-K., et al.: Off-angle illumination induced surface plasmon coupling in subwavelength metallic slits. *Opt. Express* **13**(26), 10784–10794 (2005)
- Wu, T., et al.: The sensing characteristics of plasmonic waveguide with a single defect. *Opt. Commun.* **323**, 44–48 (2014)
- Xiang, D., Li, W.: MIM plasmonic waveguide splitter with tooth-shaped structures. *J. Mod. Opt.* **61**(3), 222–226 (2014)
- Yan, S., et al.: Refractive index sensor based on a metal–insulator–metal waveguide coupled with a symmetric structure. *Sensors* **17**(12), 2879 (2017)
- Yin, J., Tian, J., Yang, R.: Investigation of the transmission properties of a plasmonic MIM waveguide coupled with two ring resonators. *Mater. Res. Express* **6**(3), 035018 (2018)
- Zafar, R., Salim, M.: Enhanced figure of merit in Fano resonance-based plasmonic refractive index sensor. *IEEE Sens. J.* **15**(11), 6313–6317 (2015)
- Zhang, Q., et al.: A subwavelength coupler-type MIM optical filter. *Opt. Express* **17**(9), 7549–7554 (2009)
- Zhang, X., et al.: Refractive index sensor based on fano resonances in plasmonic waveguide with dual side-coupled ring resonators. *Photonic Sens.* **8**(4), 367–374 (2018)
- Zhang, Z., et al.: Plasmonic refractive index sensor with high figure of merit based on concentric-rings resonator. *Sensors* **18**(1), 116 (2018)
- Zhao, H., Guang, X.G., Huang, J.: Novel optical directional coupler based on surface plasmon polaritons. *Physica E* **40**(10), 3025–3029 (2008)
- Zheng, G., et al.: Metal–insulator–metal waveguide-based band-pass filter with circular ring resonator containing Kerr nonlinear medium. *Opti.Communic.* **305**, 164–169 (2013)

Publisher's Note Springer Nature remains neutral with regard to jurisdictional claims in published maps and institutional affiliations.